AD_____

Award Number:  W81XWH-10-1-0387


TITLE:  Preclinical Testing of Combination Therapy for Malignant Tumors Arising from Neurofibromas


PRINCIPAL INVESTIGATOR:   Gregory Riggins


CONTRACTING ORGANIZATION:  Johns Hopkins University
                          Baltimore, MD 21218-2680


REPORT DATE: June 2012


TYPE OF REPORT: Revised Final


PREPARED FOR:  U.S. Army Medical Research and Materiel Command
               Fort Detrick, Maryland  21702-5012


DISTRIBUTION STATEMENT: Approved for Public Release;
                        Distribution Unlimited


The views, opinions and/or findings contained in this report are those of the author(s) and should not be construed as an official Department of the Army position, policy or decision unless so designated by other documentation.

| 1. REPORT DATE | 2. REPORT TYPE | 3. DATES COVERED |
|---|---|---|
| June 2012 | Revised Final | 1 June 2010- 31 May 2012 |

| 4. TITLE AND SUBTITLE | | 5a. CONTRACT NUMBER |
|---|---|---|
| Preclinical Testing of Combination Therapy for Malignant Tumors Arising from Neurofibromas | | |
| | | 5b. GRANT NUMBER |
| | | W81XWH-10-1-0387 |
| | | 5c. PROGRAM ELEMENT NUMBER |

| 6. AUTHOR(S) | 5d. PROJECT NUMBER |
|---|---|
| Gregory Riggins | |
| | 5e. TASK NUMBER |
| | |
| | 5f. WORK UNIT NUMBER |
| **E-Mail:** griggin1@jhmi.edu | |

| 7. PERFORMING ORGANIZATION NAME(S) AND ADDRESS(ES) | 8. PERFORMING ORGANIZATION REPORT NUMBER |
|---|---|
| Johns Hopkins University Baltimore, MD 21218-2680 | |

| 9. SPONSORING / MONITORING AGENCY NAME(S) AND ADDRESS(ES) | 10. SPONSOR/MONITOR'S ACRONYM(S) |
|---|---|
| U.S. Army Medical Research and Materiel Command Fort Detrick, Maryland 21702-5012 | |
| | 11. SPONSOR/MONITOR'S REPORT NUMBER(S) |

**12. DISTRIBUTION / AVAILABILITY STATEMENT**
Approved for Public Release; Distribution Unlimited

**13. SUPPLEMENTARY NOTES**

**14. ABSTRACT**

.
This is the final report that shows the results obtained during the funding. The aim of this study was indentify combinations of currently approved drugs that would be effective for treating MPNST. The resources attained along the first phase of this project were valuable for the subsequent drug screen performed in human MPNST cells and in vivo experiments. The inhibition of mammalian target of rapamycin (mTOR) by drugs (Rapamycin and RAD001) or RNA interference shows synergism with ionizing radiation decreasing human MPNST cell proliferation. Cell-based drug screen in combination with mTOR inhibitiors uncovers three potential candidates (toremifene, riluzole and bortezomib) with different mechanism of action. We further characterized the interaction between bortezomib, a proteasome inhibitor, and mTOR signaling inhibition in MPNST cells proliferation, cell cycle and apoptosis. Finally, dual targeting of proteasome and mTOR signaling associated with radiotherapy delay MPNST tumor growth in xenograft nude mice.

**15. SUBJECT TERMS**- MPNST, Neurofibromatosis Type 1, drug screen, mTOR signaling

| 16. SECURITY CLASSIFICATION OF: | | | 17. LIMITATION OF ABSTRACT | 18. NUMBER OF PAGES | 19a. NAME OF RESPONSIBLE PERSON USAMRMC |
|---|---|---|---|---|---|
| a. REPORT | b. ABSTRACT | c. THIS PAGE | | | 19b. TELEPHONE NUMBER (include area code) |
| U | U | U | UU | 25 | |

## Table of Contents

# INTRODUCTION

About one half of Malignant Peripheral Nerve Sheath Tumors (MPNST) arise in Neurofibromatosis Type 1 patients (NF1). *NF1* is a tumor suppressor gene normally essential for negative regulation of RAS protein and is the most common genetic alteration in MPNST. Currently, these tumors present very poor clinical prognosis, and despite the efforts to find better chemotherapy, there has been little impact on overall patient survival. Our goal was to identify new combination of FDA approved drugs that are effective in cell culture and animal models of MPNST.

# BODY

The results obtained in the first year were valuable to perform cell based drug screen and test the therapy combination *in vivo*. In the first year, we successfully developed new MPNST cells derived from surgical specimens provided by the Johns Hopkins Hospital and established MPNST xenograft mouse models. During the second year we developed two additional MPNST cells in serum containing medium derived from surgical specimens. In addition, we used a cell based drug screen to identify potential combinations with anti-proliferative effect *in vitro*. These combinations were further characterized in a detailed analysis of cell cycle profile and apoptotic markers. Finally, we tested whether this therapeutic approach shows anti-tumoral activity in preclinical model.

## Task 1 – Establishment of new MPNST cells

Surgically resected MPNST tumors were dissociated and cells were cultured in neural stem cell media made of Neurobasal medium (Invitrogen) containing the mitogenic factors EGF and FGF. We also cultured these cells in standard serum containing medium with 10% of Fetal Bovine Serum. To date, cells cultured in neural stem cells medium grew for a few passages and rapidly senesced. This might be attributed to the specific genetic background of tumors, as cultured primary cells regularly differ in cell proliferation rates and therefore in the ability to form new cell lines. Up to the present time, we have successfully grown five new MPNST cells in serum containing medium and currently have cultured these cells for several passages (Figure 1). On Figure 1 the *in vitro* characteristic growth pattern of these cells is shown. We also obtained established MPNST cells kindly provided by outside collaborators. A complete list of MPNST cells is shown on Table 1.

## Task 2 – In vivo tumor growth and characterization of MPNST cells

In order to develop a consistent *in vivo* MPNST model we implanted all available MPNST cells in athymic nude mice. MPNST cells growing in culture were trypsinized, counted and resuspended in Matrigel (BD Biosciences). $5x10^6$

cells resuspended in 100 µl of Matrigel were implanted subcutaneously in the middle portion of flanks of Athymic nude mice. Mice were observed overtime for tumor formation. Mice implanted with the cell lines STS26T and NF90-8 developed tumors 4 and 12 weeks after cell implantation, respectively. We also successfully implant the sNF96-2 and T265-2C cell lines in athymic nude mice, which developed tumors nearly 10 weeks after cell implantation.

## Task 3 – Establishment of NF1 isogenic cells

**A)    Suppression of NF1 expression in MPNST cells.** NF1 tumor suppressor loss is one of the most common genetic alterations in MPNST tumors. It is anticipated that finding a drug that shows specificity to cells lacking NF1 expression will represent a major step toward developing an efficacious therapy for MPSNT tumors. Therefore, we developed NF1 isogenic cells, which have the same genetic background and only differ on the *NF1* gene expression. To that end, we selected the NF1 positive cell STS26T and proceeded to attain the constitutive knockdown of NF1 gene. To mimic NF1 expression loss we transduced lentiviral shRNA constructs specific for *NF1* gene. The shRNA system selected was the Hairpin-pLKO.1 from the RNAi Consortium (TRC), available at the Genomics Resource core facility at JHU. We selected five independent *NF1* shRNA clones: TRCN39713, TRCN39714, TRCN39715, TRCN39716 and TRCN39717. The *NF1* hairpins are cloned into the lentiviral pLKO.1 vector. The non-targeting GFP shRNA was used as a control. Figure 2A shows the protein expression of NF1 in the MPNST cells with the shRNA (clone TRCN39716) selected from our initial screen performed by quantitative real-time PCR (*data not shown*). Next, the selected *NF1* shRNA clone was tested for their proliferation rates by Alamar Blue assay (Invitrogen). Suppression of NF1 protein expression (clone TRCN39716) was accompanied of increased cell proliferation, compared to the GFP shRNA control (Figure 2B). Therefore, we used clone TRCN39716 for the subsequent drug screening. NF1shRNA and GFPshRNA cells were subjected to various concentrations of the inhibitors: Tandutinib, Sunitinib, Rapamycin, Gefitinib and Lapatinib. Control cells were plated with DMSO, used as vehicle for drug dilutions. The drugs half inhibitory concentration (IC$_{50}$) value was calculated at 72h after drug exposure. Table 2 shows the results of the initial IC$_{50}$ assays.

**B)    NF1 ectopic expression in normal arachnoidal cells.** The *NF1* cDNA (clone 88:12) was kindly provided by Dr. F Hannan PhD (New York Medical College, Valhalla, NY) (1). The NF1 plasmid construct was double-digested with Not-I and Sal-I and the *NF1* insert was ligated into the linearized retroviral vector pBicep-CMV2 (Sigma). The resulting DNA construct was transformed and expanded in DH5-alpha cells. Empty vector pBicep-CMV2 and pBicep-CMV2-NF1 were transiently transfected into normal arachnoidal cells using Lipofectamine 2000. The level of *NF1* expression was assessed by real-time PCR. NF1 ectopic expression was increased >100 fold compared to the empty vector control (*data not shown*).

## Task 4 - Test FDA approved drug libraries to identify drug combinations that show synergistic inhibition in MPNST.

**A)    Ionizing radiation in combination with mTOR inhibitors.** The current treatments of MPNST involve surgery following radiotherapy and chemotherapy. To test if human MPNST cells proliferation is regulated by radiation *in vitro* we submitted MPNST cell to different doses of ionizing radiation. A significant reduction in cell viability was observed in a dose-dependent manner in MPNST cells after radiation (Figure 3). Since mTOR inhibition radiosensitizes soft tumor sarcoma (2), we reasoned that mTOR inhibition would synergize with radiation in MPNST cells. In addition, hyperactivation of mTOR is observed in human MPNST samples and normal cells with *NF1* overexpression (3). On the other hand, blocking mTOR signaling with Rapamycin decreased cell proliferation in MPNST cells *in vitro* and in xenograft nude mice, suggesting that mTOR signaling is critical to MPNST harboring *NF1* mutations growth (4, 5). Therefore, we first determined the half inhibitory concentration ($IC_{50}$) for Rapamycin and RAD001 (Everolimus), two mTOR inhibitors FDA approved drugs, in human MPNST cells (Figure 4, Table 3). Ionizing radiation (12 Gy) in combination with pharmacological mTOR signaling inhibition, Rapamycin or RAD001 at 25% of $IC_{50}$, significantly reduces cell proliferation when comparing with single treatment (Figure 5). Finally, to confirm that mTOR signaling interacts directly with ionizing radiation rather than an *off-target* effect of Rapamycin or RAD001, we used RNA interference-mediated mTOR gene silencing in human MPNST cells. Using Western blot analysis we confirmed the down-regulation of mTOR protein expression induced by two different RNA interference sequences (Figure 6A). mTOR gene silencing plus radiation (12 Gy) diminished MPNST cell proliferation (Figure 6B). These experiments confirm by two different approaches, pharmacological and genetically, that mTOR synergism with radiation in MPNST cells.


**B)    Screening of 542 FDA approved compounds indentifies drugs that show synergy with mTOR inhibitors.** Cell-based screen is a valuable tool to identify novel compound with anti-tumoral activity. Notably, this method accelerates drug discovery for neglected or rare diseases. We used two FDA approved libraries (NINDS: National Institute of Neurological Disorders and Stroke; and NCI: National Cancer Institute – Approved Oncology Drug Set III) and analysis cell proliferation was performed in combination with Rapamycin or RAD001 at 25% of their $IC_{50}$. Table 4 describes the protocol used in the cell-based screen (6). In brief, NF90.8 cells were seeded (1,000 cells/well) in 96-well plates, allowed to attach for 1 day, treated with libraries compounds and Rapamycin or RAD001, and analyzed for cell viability daily with a fluorescence-based assay (Alamar Blue, Invitrogen). We screened a collection of 542 compounds (4 µM) in combination with mTOR inhibitors (Rapamycin or RAD001 at 25% of $IC_{50}$) (Figure 7). Twenty two compounds exhibited synergism with mTOR inhibitors, decreasing more than 50% of cell viability when combined with mTOR inhibitors. We selected 10 of these 22 compounds for further study, based on their ability to decrease cell viability in two additional human MPNST cell lines (sNF96.2 and T265-2C cells). Upon retesting, 3 of 10 compounds showed consistent evidence of selective toxicity in MPNST cells (table 5).

Recently, a new study was presented of tumor cell lines harboring *NF1* mutation showing a strong sensitivity to bortezomib, a proteasome inhibitor used to treat multiple myeloma and lymphoma (7, 8). This finding has an important clinical implication, since mutated cancer genes are potent biomarkers for responses to targeted agents. Therefore, we focused on bortezomib and further characterized the interaction between bortezomib and mTOR in MPNST cells. Bortezominb reduced significantly the chymotrypsin-like activity of the 20S proteasome in a fluorescence cell-based assay (Proteasome-Glo, Promega) in NF90-8 and T265-2C cells (Figure 8). Testing the half inhibitory concentration ($IC_{50}$) for bortezomib in combination with different doses of Rapamycin or RAD001, we observed a consistent decrease in the $IC_{50}$ values for bortezomib (Figure 9 and Table 6). Bortezomib at 25% of $IC_{50}$ reduces the $IC_{50}$ for Rapamycin or RAD001 in NF90.8 and T265-2C (*data not shown*).

As showed in Figure 10, the synergy between mTOR inhibitors and bortezomib was confirmed using the Chou-Talalay algorithm for drug combination (9). The calculation analysis results in a combination index (CI) which offers a quantitative definition for additive effect (CI = 1), synergism (CI < 1), and antagonism (CI > 1) in drug combinations studies (9). The Chou-Talalay algorithm helps us answer the following primary questions: (*a*) Are there any synergisms? (*b*) How much synergism? (*c*) Synergism at what dose levels? Hence, as showed in figure 10, using the Chou-Talalay algorithm we determined the best concentration of bortezomib and mTOR inhibitors for further combinations with radiation.

**C)     Dual targeting of proteasome and mTOR signaling associated with radiotherapy in MPNST cells *in vitro*.**

Drug combination (RAD001 and bortezomib) associated with ionizing radiation reduces human MPNST cell viability (Figure 11). Cell cycle analysis using propidium iodide DNA staining reveals the enhancement of SubG1 fraction after drug combination and radiation in NF90.8 and T265-2C cell line (Table 7). The augmented SubG1 fraction strongly suggested that these cells are trigged to apoptosis after drug treatment. Therefore, we performed a protein expression of apoptosis regulators, as well cleaved-PARP, an apoptotic marker and one of the major targets of caspase-3. Although drug combination and radiation differently regulates cell proliferation, protein expression suggested that radiation induces a more substantial alteration in protein expression, decreasing the anti-apoptotic protein BCL-xL and enhancing the pro-apoptotic protein BAX and the apoptosis marker cleaved-PARP (Figure 12).

**Task 5 - Dual targeting of proteasome and mTOR signaling associated with radiotherapy in MPNST cells *in vivo*.**

**A)     Small Animal Radiation Research Platform is a suitable method to study the effect of ionizing radiation in MPNST xenograft tumor.** Tumor xenotransplantation in nude mice is a robust model to assay the efficacy of drug

and radiation treatments *in vivo*. Here, we first tested the influence of local ionizing radiation in NF90.8 and sNF96.2 cells implanted in the left and right flank in female nude mice. Ten days after tumor implantation ionizing radiation was performed in tumor using Small Animal Radiation Research Platform (SARRP), which mimics the isocentric external-beam treatment machine used to deliver image-guided radiotherapy for humans (10). Right tumor in xenograft nude mice was irradiated, while the left tumor was used as control. In brief, a CT-SPOT with 2.3 mm (Beeley) was used to identify the tumor in the animal microcomputer tomography (CT) systems. Next, the tumor was subjected to 20 Gy in a single dose 4 mm below the mouse skin (Figure 13A). Figure 13B shows a representative image of sNF96.2 and NF90.8 obtained in the i*n vivo* animal imaging system (Xenogen IVIS) 11 weeks after tumor implantation. Irradiated tumors presented slower growth than control, showing that radiation is a suitable strategy to test drug combination plus radiation in MPNST growth in xenograft mice (Figure 13C).

**B)** ***In vivo* toxicity test of drug combination.** Next, we tested whether bortezomib associated with RAD001 promotes general toxicity in mice. Bortezomib was administered intraperitoneally twice per week at 50% (0.65 mg/m$^2$), 75% (0.97 mg/m$^2$), and 100% (1.3 mg/m$^2$) of MTD in combination with RAD001 administrated orally 5 times per week at 75% (1.5 mg/kg) of MTD. Body mass was assessed three times a week and showed that drug combination was well tolerated with no significant weight loss in none of the animal groups (Figure 14A).

**C)** **Drug combination associated with radiation decrease MPNST tumor growth in xenograft nude mice.** Encouraged by our results from drug combination *in vitro* and the well-tolerated drug combination *in vivo* we tested the efficacy of treatment of RAD001 (1.5 mg/Kg; 5 days/week) plus bortezomib (1.3 mg/m$^2$; 2 days/week) associated with a single dose of local ionizing radiation (10 Gy) in MPNST tumor growth in xenograft implanted nude mice. Female nude mice bearing NF90.8 tumor in the right flank were randomized in 6 groups: Control (n=4); bortezomib + RAD001 (n=4); Ionizing radiation (RT) (n=5); RT + bortezomib (n=5); RT + RAD001 (n=5); and RT + bortezomib + RAD001 (n=5). As showed in figure 14B, after 9 weeks of treatment all combination therapy decreased tumor growth, with a pronounced effect in the group RT + bortezomib + RAD001, suggesting that multiples signaling pathways should be target to decrease MPNST growth *in vivo*. Therefore, our study revealed promising synergistic effect between mTOR inhibitors and bortezomib.

## KEY RESEARCH ACCOMPLISHMENTS

1. We established new MPNST cell lines from surgical specimens.
2. We developed NF1 isogenic cells appropriated for screening of anti-neoplastic FDA approved drugs and also to understand the molecular mechanism associated with NF1 tumorigenesis.
3. We have identified a new therapy combination that reduces MPNST cell growth *in vitro* and *in vivo*.

## REPORTABLE OUTCOMES

We indentify FDA approved drugs that are currently in use in clinical practice and in combination are more effective in MPNST growth suppression than single drug treatment.

## CONCLUSION

Our investigation shows that mTOR inhibitor in combination with radiation and bortezomib are more efficient in diminishing human MPNST cells growth *in vitro and in vivo*, compared to either treatment alone. These results might provide a clinical relevant therapeutic option suggesting a strong rationale for treatment of human MPNTs.

## REFERENCES

1.  Hannan F, Ho I, Tong JJ, et al. 2006 Effect of neurofibromatosis type I mutations on a novel pathway for adenylyl cyclase activation requiring neurofibromin and Ras. Hum Mol Genet. **15**:1087-1098.
2.  Murphy JD, Spalding AC, Somnay YR, et al. 2009 Inhibition of mTOR radiosensitizes soft tissue sarcoma and tumor vasculature. Clin Cancer Res. **15**:589-596.
3.  Zou CY, Smith KD, Zhu QS, et al. 2009 Dual targeting of AKT and mammalian target of rapamycin: a potential therapeutic approach for malignant peripheral nerve sheath tumor. Mol Cancer Ther. **8**:1157-1168.
4.  Johannessen CM, Johnson BW, Williams SM, et al. 2008 TORC1 is essential for NF1-associated malignancies. Curr Biol. **18**:56-62.
5.  Bhola P, Banerjee S, Mukherjee J, et al. 2010 Preclinical in vivo evaluation of rapamycin in human malignant peripheral nerve sheath explant xenograft. Int J Cancer. **126**:563-571.
6.  Inglese J, Shamu CE, Guy RK 2007 Reporting data from high-throughput screening of small-molecule libraries. Nat Chem Biol. **3**:438-441.
7.  Garnett MJ, Edelman EJ, Heidorn SJ, et al. 2012 Systematic identification of genomic markers of drug sensitivity in cancer cells. Nature. **483**:570-575.
8.  Hideshima T, Richardson PG, Anderson KC 2011 Mechanism of action of proteasome inhibitors and deacetylase inhibitors and the biological basis of synergy in multiple myeloma. Mol Cancer Ther. **10**:2034-2042.
9.  Chou TC 2010 Drug combination studies and their synergy quantification using the Chou-Talalay method. Cancer Res. **70**:440-446.
10. Wong J, Armour E, Kazanzides P, et al. 2008 High-resolution, small animal radiation research platform with x-ray tomographic guidance capabilities. Int J Radiat Oncol Biol Phys. **71**:1591-1599.
11. Kraniak JM, Sun D, Mattingly RR, et al. 2010 The role of neurofibromin in N-Ras mediated AP-1 regulation in malignant peripheral nerve sheath tumors. Mol Cell Biochem. **344**:267-276.

**12.** Im JS, Tapinos N, Chae GT, et al. 2006 Expression of CD1d molecules by human schwann cells and potential interactions with immunoregulatory invariant NK T cells. J Immunol. **177**:5226-5235.

**13.** Fieber LA, Gonzalez DM, Wallace MR, Muir D 2003 Delayed rectifier K currents in NF1 Schwann cells. Pharmacological block inhibits proliferation. Neurobiol Dis. **13**:136-146.

## SUPPORTING DATA
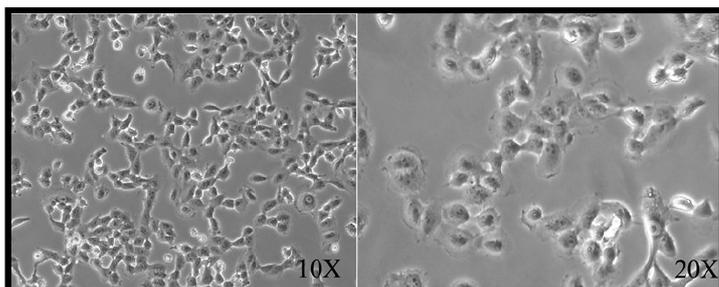


**Figure 1. MPNST cell morphology characteristic of MPNST cells growing in culture**. The 2010-013 cells growing in monolayer are observed.

**Table 1. MPNST cells established at Johns Hopkins and obtained from outside collaborators.**

| MPNST Cell | Source | Reference |
|---|---|---|
| 2010-013 | Johns Hopkins Hospital | Present study |
| 2011-005 | Johns Hopkins Hospital | Present study |
| 2011-007 | Johns Hopkins Hospital | Present study |
| 2011-008 | Johns Hopkins Hospital | Present study |
| JHH528 | Johns Hopkins Hospital | Present study |
| NF90.8 | Dr Michael Tainsky, Wayne University, Detroit, MI | (11) |
| ST88-14 | Dr Michael Tainsky, Wayne University, Detroit, MI | (11) |
| STS26T | Dr Steven Porcelli, Albert Einstein College of Medicine, Bronx, NY | (12) |
| T265-2C | Dr Steven Porcelli, Albert Einstein College of Medicine, Bronx, NY | (12) |
| sNF96.2 | ATCC (cat n. CRL-2884) | (13) |

**A** Western Blotting



NF1 — 250 kDa

α-TUBULIN — 52 kDa

(shRNA-GFP, shRNA-NF1)

**B** Cell viability



- ■ shRNA-GFP
- ■ shRNA-NF1

Y-axis: Flourescence intensity ($10^4$)
X-axis: Time (days)

*** at days 1, 2, 3, 4
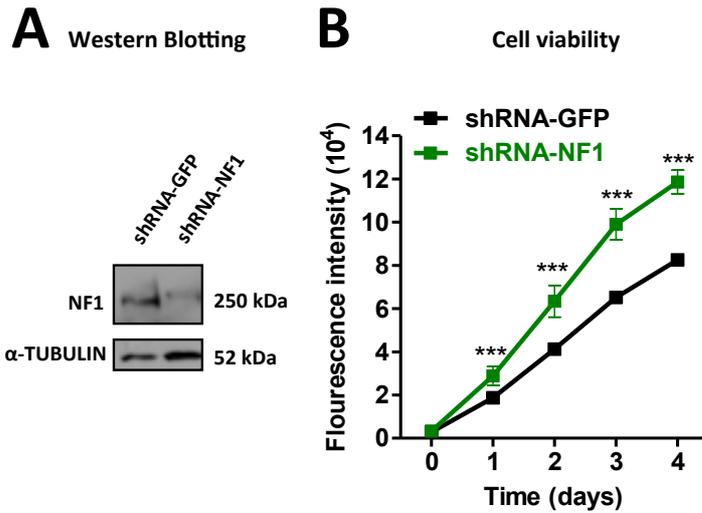
**Figure 2. Establishment of a NF1 isogenic cell line.** (**A**) Constitutive NF1 knockdown in STS26T cell line was analyzed by Western Blotting. Fifty (μg) of total protein lysate was separated by SDS-PAGE and immunoblot was performed against NF1 (sc-67) and α-TUBULIN (B7) (all from Santa Cruz Biothecnology). (**B**) STS26T shRNA-GFP and STS26T shRNA-NF1 were seeded (1000 cells/well) in quadruplicate in 96-well plate and cell proliferation were assessed by Alamar blue assay. *** *P<0,001 vs STS26T shRNA-GFP.*

**Table 2. IC$_{50}$ values for MPNST cells with constitutive NF1 knockdown compared to the control (shRNA-GFP)**

| Compounds | Target | shRNA-GFP | shRNA-NF1 |
|---|---|---|---|
| | | IC$_{50}$ (μM) / $R^2$ | IC$_{50}$ (μM) / $R^2$ |
| Tandutinib | PDGFR, FLT3, c-Kit | 120 / 0.93 | 52 / 0.90 |
| Lapatinib | EGFR, Erb/Her | 7.5 / 0.98 | 6 / 0.91 |
| Gefitinib | EFGR | 20 / 0.93 | 16 / 0.99 |
| Rapamycin | mTOR | 13 / 0.96 | 13 / 0.91 |
| Sunitinib | VEGF, PDGFβ, c-Kit | 11.5 / 0.98 | 16 / 0.93 |
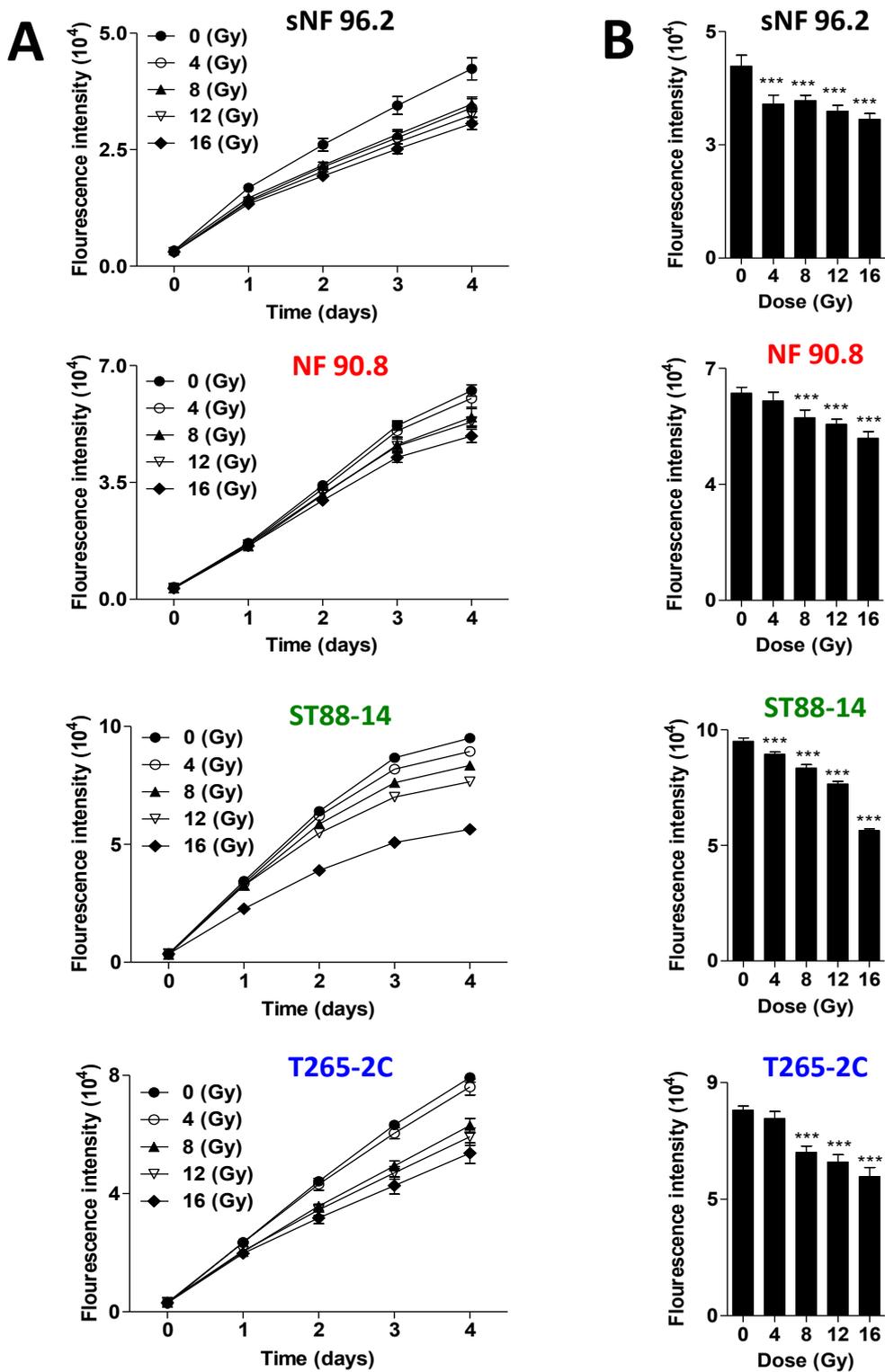
**Figure 3. Ionizing radiation inhibits proliferation in MPNST cells.** (**A**) Human MPNST cells were submitted to different doses of ionizing radiation Gammacell 1000 (2.24 Gy/min; radiation source: Caesium[137]), seeded (1000 cells/well) in quadruplicate in 96-well plate and cell proliferation were assessed by Alamar blue assay. (**B**) Graphic representation of growth 96 hours after ionizing radiation. The data are the mean ± standard deviation. *** *p<0.001* vs 0 Gy.
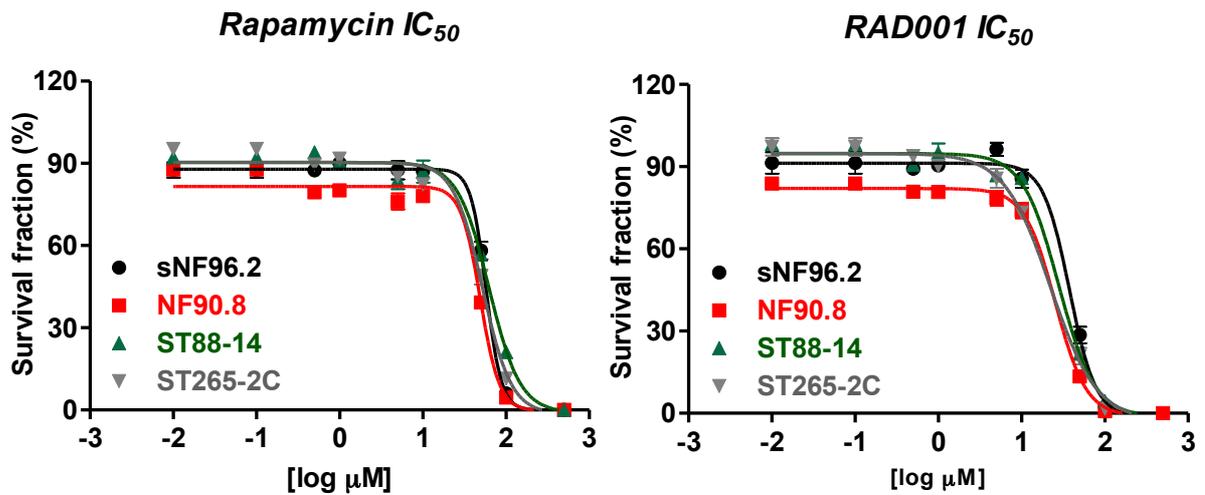
**Figure 4. IC$_{50}$ values in response to Rapamycin or RAD001 in human MPNST cell lines.** MPNST cells were seeded (1000 cells/well) in triplicate in 96-well plate, treated with different concentrations of Rapamycin or RAD001 and analyzed by Alamar blue assay. The drug half inhibitory concentration (IC$_{50}$) value was calculated at 72 hours after drug exposure. IC$_{50}$ assays were analyzed using GraphPad Prism software. Data are represented as average ± standard deviation of three independent experiments performed in triplicate.

**Table 3. IC$_{50}$ values in response to mTOR inhibitors.**

| | IC$_{50}$ (µM) | |
|---|---|---|
| Cell line | Rapamycin | RAD001 |
| sNF96.2 | 53.6 ± 3.7 | 23.7 ± 12.5 |
| NF90.8 | 50.3 ± 4.0 | 20.9 ± 6.2 |
| ST88-14 | 54.4 ± 8.1 | 25.8 ± 6.3 |
| T265-2C | 42.3 ± 8.8 | 19.3 ± 3.0 |
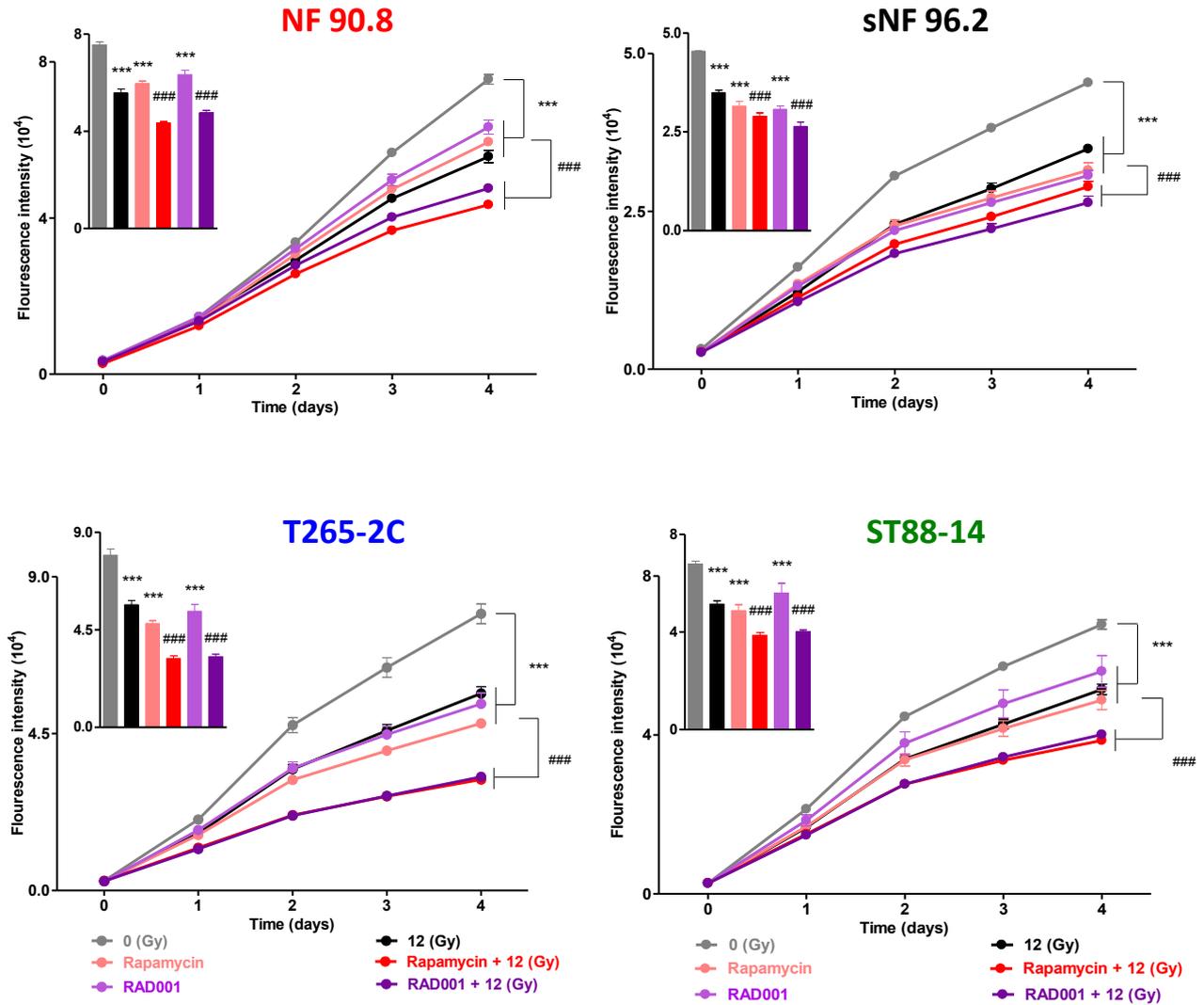
**Figure 5. Anti-proliferative effects of in mTOR inhibitor and ionizing radiation in MPNST cell lines.** (**A**) Human MPNST cells were submitted to ionizing radiation (12 Gy) (Gammacell 1000; 2.24 Gy/min; radiation source: Caesium[137]), seeded (1000 cells/well) in quadruplicate in 96-well plate, and treated with Rapamycin (25% of $IC_{50}$) or RAD001 (25% of $IC_{50}$) and cell growth were assessed by Alamar blue assay. * $p<0.05$ vs control; ** $p<0.01$ vs control; *** $p<0.001$ vs control; # $p<0.05$ vs 12 Gy; ## $p<0.01$ vs 12 Gy; ### $p<0.001$ vs 12 Gy.
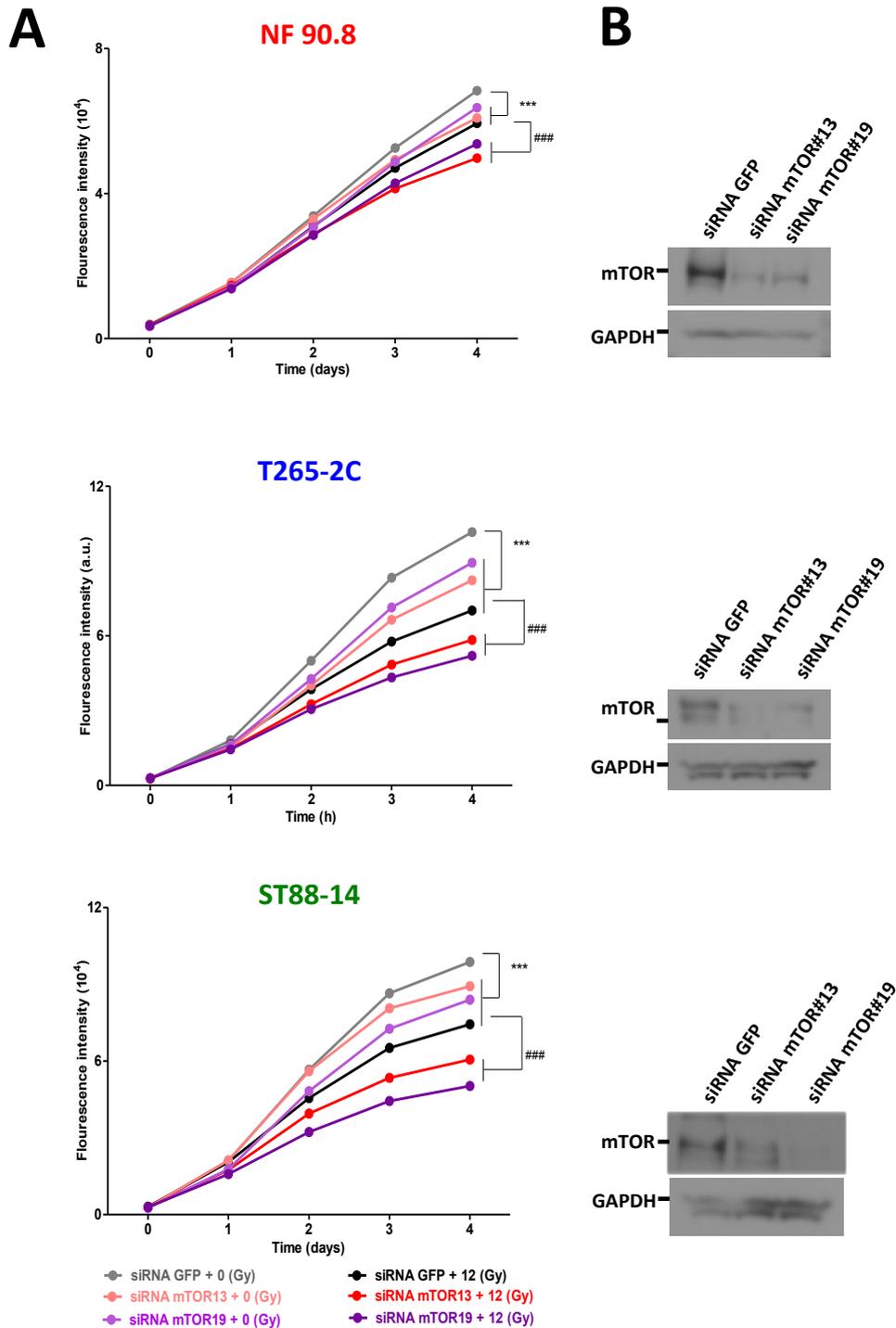
**Figure 6. Anti-proliferative effects of in mTOR silence and ionizing radiation in MPNST cell lines.** (**A**) Human MPNST cells were transfected with siRNA-GFP, siRNA mTOR13, or siRNA mTOR19 (10 nM for NF90.8 and 5 nM for T265-2C and ST88-14 cells), submitted to ionizing radiation (12 Gy) (Gammacell 1000; 2.24 Gy/min; radiation source: Caesium[137]), seeded (1000 cells/well) in 96-well plate, and cell growth were assessed by Alamar blue assay. *\*\* p<0.01 vs control; \*\*\* p<0.001 vs control; ## p<0.01 vs 12 Gy; ### p<0.001 vs 12 Gy.* (**B**) Total protein lysates (50 μg) from MPNST cells was separated by SDS-PAGE and analyzed by Western blot for mTOR and GAPDH, which was used as a loading control.

**Table 4. Cell-based screening protocol.**

| Step | Parameter | Values | Description |
|---|---|---|---|
| 1 | Plate cell | 1000 cells/well in 96 well plate | NF96.8 human MPNST cell line |
| 2 | Dilute NINDS and NCI libraries | 400 µM final concentration | Use DMSO as a diluent |
| 3 | Add libraries compounds | 4 µM final concentration | |
| 4 | Add Alamar Blue reagent | 20 µL | Alamar Blue reagent (Invitrogen) |
| 5 | Assay readout | 72h after treatment | Analysis the fluorescence intensity in Victor-3 plate reader (Perkin-Elmer) |
| 6 | Data analysis | Results express as fold change vs DMSO group | Use Excel spreadsheets |
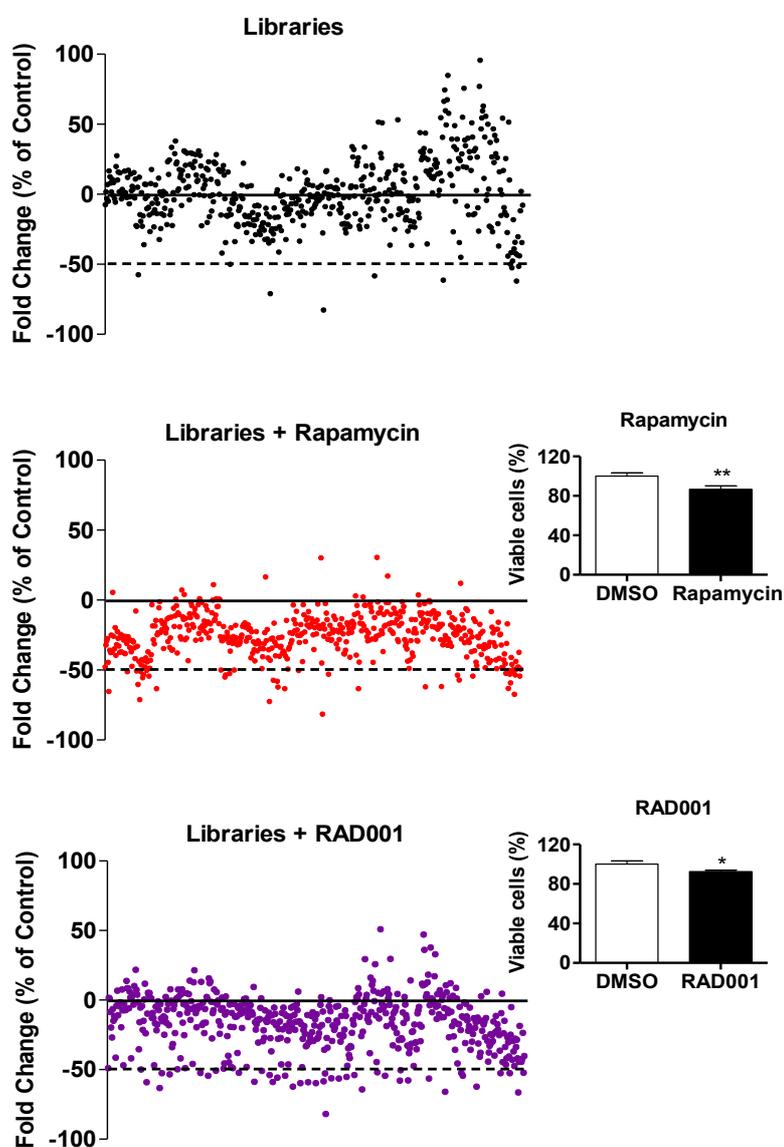


**Figure 7. Cell-based drug screen identify compound with synergistic effect with mTOR inhibitors.** (**A**) Cell-based screening was performed as described in Table 4. Inset shows the effect of mTOR inhibitors in cell proliferation. Each dot represents one compund. Data represented as fold change vs. control group.

**Table 5. IC$_{50}$ values to test the synergism between hits and mTOR inhibitors.**

| NF90.8 | | | | |
|---|---|---|---|---|
| Compounds | Target(s) | Drug (μM)/R$^2$ | Drug + Rapamycin (25% of IC$_{50}$) (μM)/R$^2$ | Drug + RAD001 (25% of IC50) (μM)/R$^2$ |
| Saquinavir | protease inhibitor | 46.6/0.99 | 45.2/0.97 | 48.4/0.99 |
| Ifenprodil | N-methyl-d-aspartate (NMDA) receptors | 198.3/0.98 | 267.70.98 | 187.6/0.96 |
| Rosiglitazone | PPAR gamma agonist | 576.2/0.84 | 1150/0.94 | 684.5/0.89 |
| DCA | pyruvate dehydrogenase kinase | >1000 | ND | ND |
| **Toremifene** | **estrogen receptor modulator** | **34.6/0.99** | **19.0/0.97** | **20.1/0.99** |
| **Riluzole** | **inhibitor of glutamate release** | **91.4/0.99** | **72.7/0.94** | **72.7/0.96** |
| Lapatinib | EGFR and ERBB2 | 9.6/0.98 | 16.0/0.97 | 12.8/0.98 |
| Vandetanib | EGFR, RET, VEGFR | 59.4/0.97 | 60.5/0.94 | 62.8/0.96 |
| Pazopanib | VEGFR, PDGF, c-KIT | 20.1/0.97 | 44.4/0.93 | 37.3/0.93 |

| T265-2C | | | | |
|---|---|---|---|---|
| Compounds | Target(s) | Drug (μM)/R$^2$ | Drug + Rapamycin (25% of IC$_{50}$) (μM)/R$^2$ | Drug + RAD001 (25% of IC50) (μM)/R$^2$ |
| **Toremifene** | **estrogen receptor modulator** | **22.6/0.99** | **18.1/0.99** | **21.0/0.99** |
| **Riluzole** | **inhibitor of glutamate release** | **106.5/0.96** | **80.9/0.96** | **119.3/0.95** |

| sNF96.2 | | | | |
|---|---|---|---|---|
| Compounds | Target(s) | Drug (μM)/R$^2$ | Drug + Rapamycin (25% of IC$_{50}$) (μM)/R$^2$ | Drug + RAD001(25% of IC50) (μM)/R$^2$ |
| **Toremifene** | **estrogen receptor modulator** | **22.1/0.99** | **12.9/0.97** | **11.2/0.99** |
| **Riluzole** | **inhibitor of glutamate release** | **97.3/0.84** | **94.5/0.97** | **97.9/0.97** |

Half inhibitory concentration was analyzed as describe in figure 4. ND: not determine. DCA: Dichoroacetate.
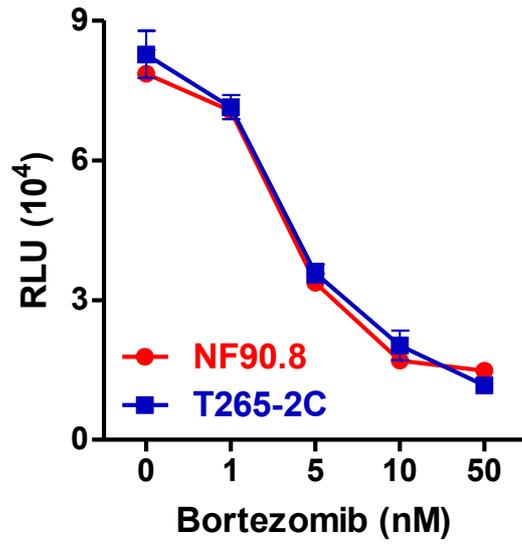
**Figure 8. Bortezomib inhibits proteasome activity in MPNST cells.** NF90.8 and T265-2C cells were seeded (10,000 cells/well) in triplicate in 96-well plate, treated with different concentrations of bortezomib and 4 hours after treatment chymotrypsin-like activity of the 20S proteasome was measured in a fluorescence cell-based assay as recommended by manufacturer (Proteasome-Glo, Promega). RLU: Relative light units.
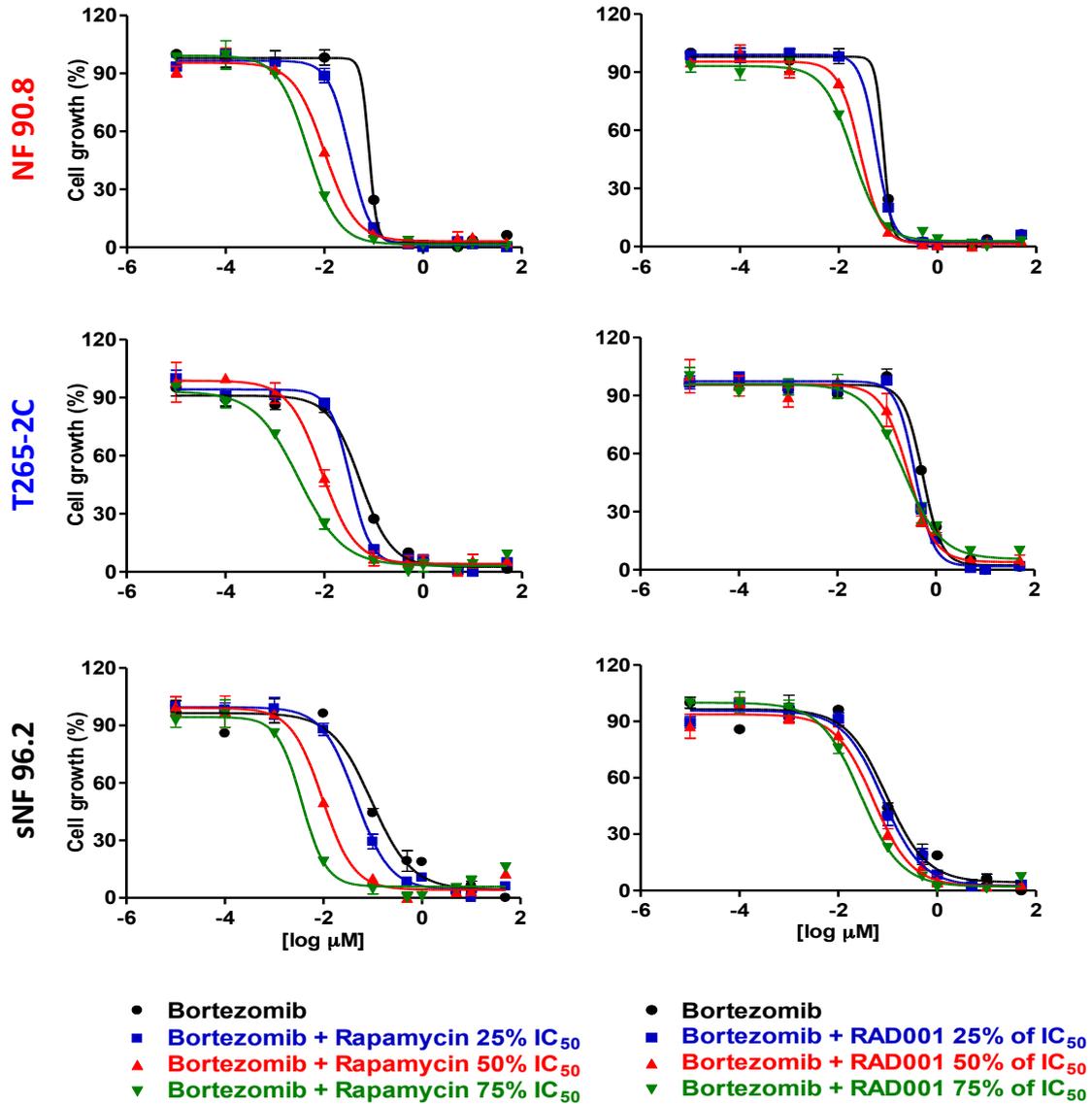
**Figure 9. IC$_{50}$ values in response to bortezomib in combination with different concentrations of Rapamycin or RAD001 in human MPNST cell lines.** NF90.8 and T265-2C cells were seeded (1000 cells/well) in triplicate in 96-well plate, treated with different concentrations of bortezomib plus rapamycin or RAD001 at the indicated concentration and cell growth was analyzed by Alamar blue assay. The drug half inhibitory concentration (IC$_{50}$) value was calculated at 72 hours after drug exposure. IC$_{50}$ assays were analyzed using GraphPad Prism software.

**Table 6. IC$_{50}$ values in response to bortezomib plus mTOR inhibitors.**

| | | MPNST cell lines | | |
|---|---|---|---|---|
| | | NF90.8 (nM) | T265-2C (nM) | sNF96.2 (nM) |
| Control | - | 80.5 | 53.7 | 95.1 |
| Rapamycin | 25 | 32.8 | 32.9 | 45.5 |
| (% of IC$_{50}$) | 50 | 10.1 | 8.9 | 9.6 |
| | 75 | 4.6 | 3.0 | 3.6 |
| RAD001 | 25 | 57.8 | 37.0 | 79.4 |
| (% of IC$_{50}$) | 50 | 27.2 | 27.5 | 51.7 |
| | 75 | 19 | 22.0 | 28.2 |



**Figure 10. Synergistic activity of mTOR inhibitors and bortezomib in MPNST cells.** NF90.8 was treated as described in figure 9 and combination index was calculated using the method of Chou and Talalay.
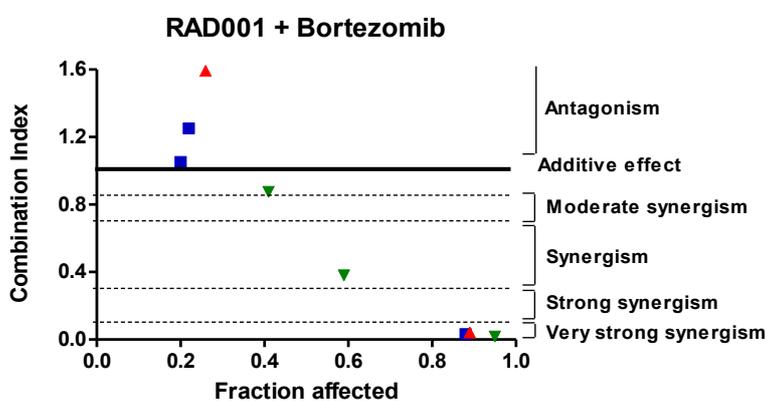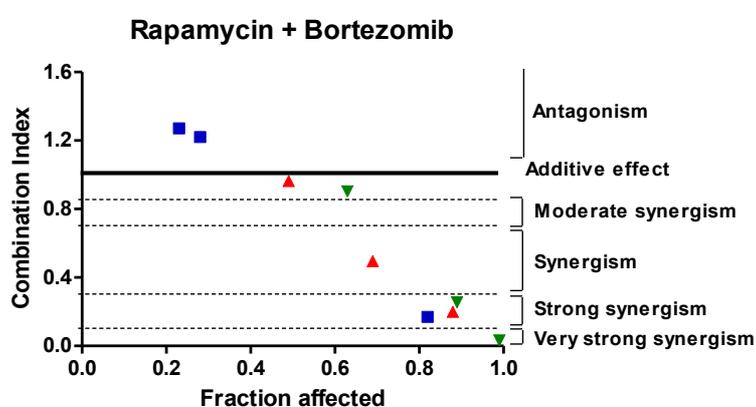
■ **Bortezomib + mTOR inhibitor 25% IC$_{50}$**
▲ **Bortezomib + mTOR inhibitor 50% IC$_{50}$**
▼ **Bortezomib + mTOR inhibitor 75% IC$_{50}$**
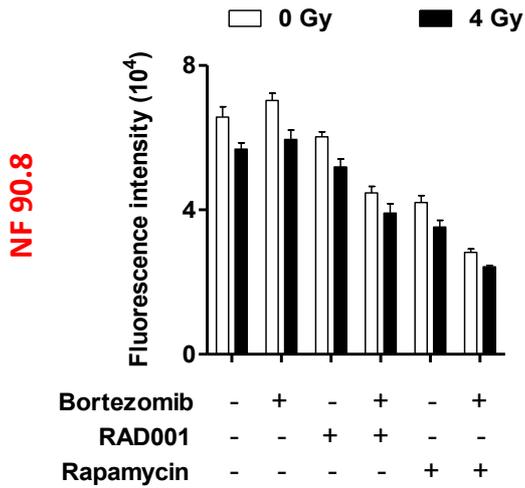
**Figure 11. Drug combination in association with radiation decreases MPNST cell viability**. MPNST cells were submitted to ionizing radiation (4 Gy) (Gammacell 1000; 2.24 Gy/min; radiation source: Caesium[137]), seeded (1000 cells/well) in quadruplicate in 96-well plate, treated with bortezomib (5nM) plus Rapamycin (50% of $IC_{50}$) or RAD001 (50% of $IC_{50}$) and after 96 hours cell growth was assessed by Alamar blue assay.

|  |  | 0 Gy |  |  |  | 2 Gy |  |  |
|---|---|---|---|---|---|---|---|---|
| Bortezomib | - | - | + | + | - | - | + | + |
| RAD001 | - | + | - | + | - | + | - | + |
| PARP | | | | | | | | |
| Cleaved PARP | | | | | | | | |
| BAX | | | | | | | | |
| BCL-xL | | | | | | | | |
| GAPDH | | | | | | | | |
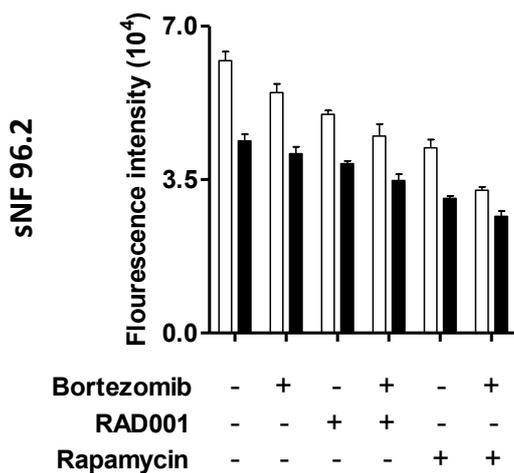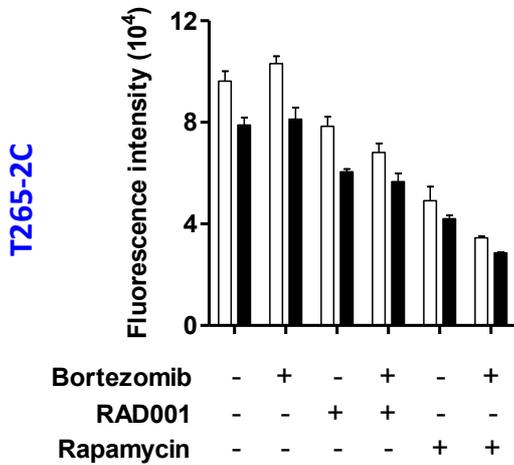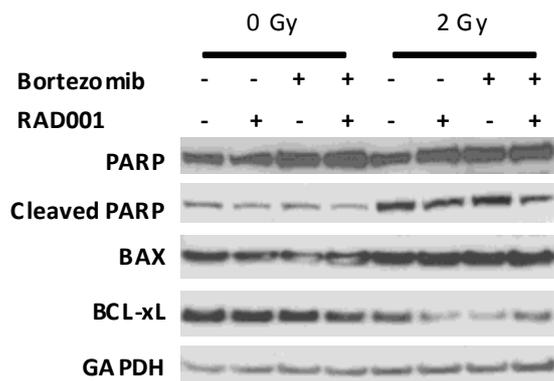
**Figure 12. Drug combination in association with radiation regulates apoptotic proteins.** NF90.8 cell line was submitted to ionizing radiation (2 Gy) (Gammacell 1000; 2.24 Gy/min; radiation source: Caesium[137]), treated with bortezomib (5 nM) plus RAD001 (50% of $IC_{50}$) and after 48 hours total protein lysates cells were separated by SDS-PAGE and analyzed by Western blot for PARP, cleaved-PARP, BAX, BCL-xL and GAPDH, which was used as a loading control.

**Table 7. Drug combination associated with ionizing radiation regulates cell cycle in MPNST cells.**

| | | NF90.8 | | | |
|---|---|---|---|---|---|
| | | *SubG1* | *G0/G1* | *S* | *G2/M* |
| 0 Gy | Control | 8 ± 0.9 | 42 ± 1.8 | 23 ± 2.9 | 27 ± 0.7 |
| | Bortezomib | 8 ± 0.6 | 47 ± 0.2 | 22 ± 0.7 | 23 ± 1.1 |
| | RAD001 | 4 ± 1.1 | 59 ± 0.8 | 18 ± 1.9 | 18 ± 2.0 |
| | Combination | 16 ± 1.1 | 31 ± 0.7 | 15 ± 1.1 | 38 ± 0.2 |
| 2 Gy | Control | 8 ± 0.3 | 50 ± 1.7 | 17 ± 0.8 | 26 ± 1.6 |
| | Bortezomib | 14 ± 3.3 | 41 ± 0.9 | 19 ± 0.6 | 27 ± 2.8 |
| | RAD001 | 5 ± 0.5 | 50 ± 1.0 | 18 ± 2.1 | 27 ± 1.0 |
| | Combination | 22 ± 4.7 | 33 ± 2.4 | 14 ± 0.9 | 31 ± 1.7 |

| | | T265-2C | | | |
|---|---|---|---|---|---|
| | | *SubG1* | *G0/G1* | *S* | *G2/M* |
| 0 Gy | Control | 5 ± 1.7 | 63 ± 1.1 | 13 ± 0.2 | 19 ± 0.8 |
| | Bortezomib | 8 ± 1.8 | 48 ± 1.7 | 11 ± 1.4 | 33 ± 1.8 |
| | RAD001 | 1 ± 0.4 | 73 ± 0.4 | 11 ± 0.5 | 15 ± 0.6 |
| | Combination | 13 ± 1.4 | 31 ± 1.0 | 12 ± 1.1 | 43 ± 1.2 |
| 2 Gy | Control | 4 ± 0.5 | 59 ± 1.1 | 14 ± 1.1 | 23 ± 0.3 |
| | Bortezomib | 14 ± 1.2 | 41 ± 2.2 | 15 ± 4.7 | 31 ± 4.1 |
| | RAD001 | 3 ± 0.5 | 70 ± 1.1 | 8 ± 1.6 | 19 ± 0.6 |
| | Combination | 18 ± 1.4 | 32 ± 2.5 | 14 ± 7.5 | 36 ± 6.6 |

NF90.8 and T265-2C cell were submitted to ionizing radiation (2 Gy) (Gammacell 1000; 2.24 Gy/min; radiation source: Caesium[137]), treated with bortezomib (5 nM) plus RAD001 (50% of $IC_{50}$) and after 48 hours cells were stained with propidium iodide and analyzed in flow cytometry (Facs Calibur, BD Bioscience)
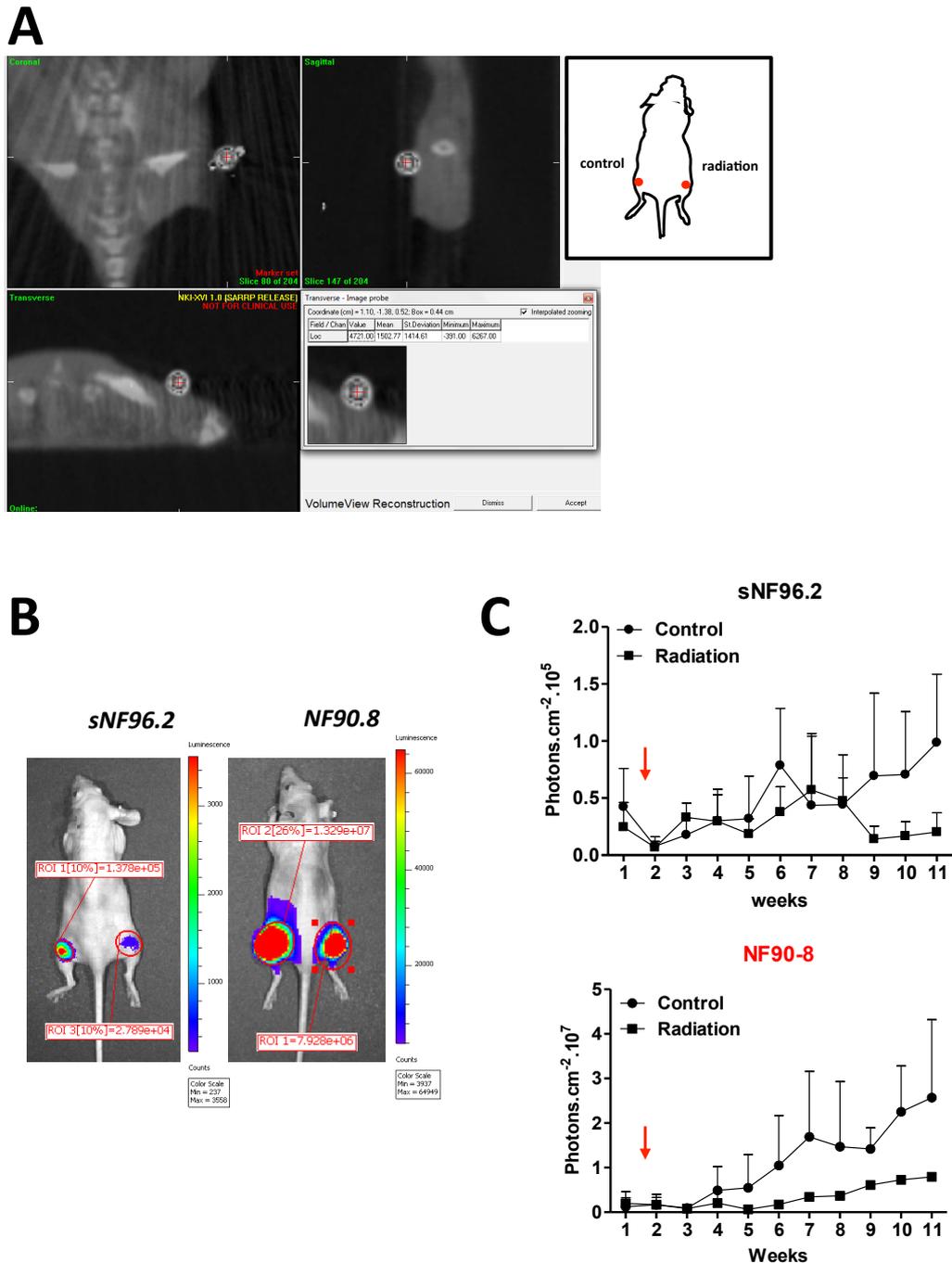
**Figure 13.** *In vivo* **radiation and MPNST xenograft tumor growth in nude mice.** (**A**) A representative picture showing CT-SPOT to identify the tumor in the animal microcomputer tomography (CT) systems. (**B**) Xenogen Ivis imaging system showing representative nude mice implanted with sNF96.2 or NF90.8 human MPNST cell lines. ROI: region of interesting showing luminescence quantification. (**C**) Tumor growth curve assessed by non-invasive luminescence *in vivo* assay in xenograft MPNST models. Arrow indicates the single dose of radiation (20 Gy).

# A
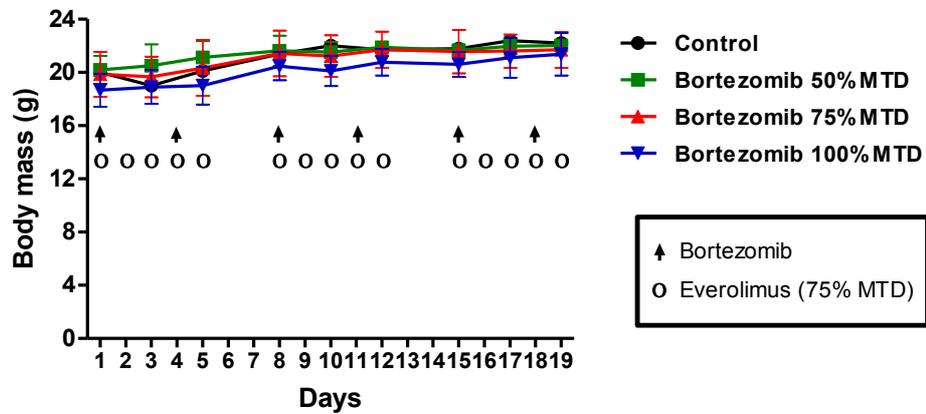


# B
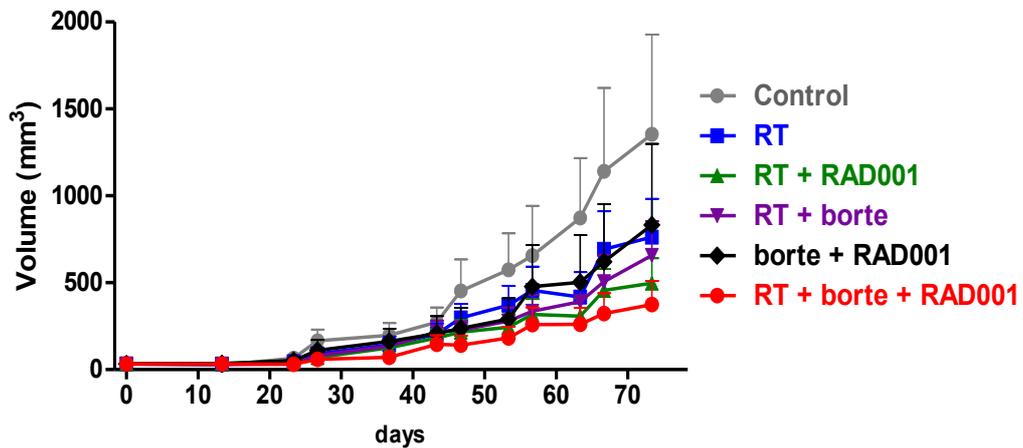


**Figure 14. Toxicity assay and drug combination associated with ionizing radiation in MPNST xenograft tumor in nude mice.** (**A**) Nude mice were randomized in four groups and drugs were administered as described in the figure. Body mass was measured three times per week. (**B**) NF90.8 tumor was implanted in nude mice and tumor volume was measured over time.